OPEN ACCESS

Kashf Journal of Multidisciplinary Research
Vol: 03 - Issue 04 (2026)
P-ISSN: 3007-1992 E-ISSN: 3007-200X
https://kjmr.com.pk

GREEN SYNTHESIS OF GRAPHENE-BASED AEROGELS FOR ULTRA-HIGH-CAPACITY ELECTROMAGNETIC INTERFERENCE SHIELDING

Ghulam Qadir Samtio[1], Faheem Ahmed[2], Deedar Ali Jamro[3], Mir Muhammad[4], Zubeda Nangrejo[5], Zaheer Hussain Abbasi[6]

[1, 2, 3, 5, 6] *Department of Physics and Electronics, Shah Abdul Latif University Khairpur, Sindh, Pakistan.*

[4] *National Center of Excellence Analytical chemistry University of Sindh, Jamshoro, Pakistan.*

[*] ***Corresponding Author:*** (samtiogq044@gmail.com)

DOI:(*https://doi.org/10.71146/kjmr905*)

Article Info

Abstract

The design of lighter and more efficient EMIs shielding materials is becoming more critical than ever in current times. In this paper, we report an environmental-friendly approach to the fabrication of reduced graphene oxide (rGO) aerogel via the use of Camellia sinensis (green tea) leaves as a bio-reductant. The polyphenolic extracts reduce the oxygen-containing functional groups from the surface of graphene oxide allowing self-assembled formation of three-dimensional porous structure without any hazardous chemicals. The produced ultralightweight (5-20 mg/cm^3) aerogels show high electrical conductivity up to 48.2 S/m and outstanding EMI shielding effectiveness between 50.5-72.4 dB in the X-band (8.2-12.4 GHz) with the dominance of the absorption process. The obtained specific EMI shielding effectiveness was about 2400 $dB \cdot cm^3/g$. The performance was much higher compared to the commonly used metal foils and chemically reduced graphene composites.

Keywords:
Graphene aerogel, green synthesis, EMI shielding, Camellia sinensis (green tea) extract.

1 Introduction

Due to the fast-growing development of contemporary electronic appliances, wireless communication equipment, and high-frequency techniques, there has been a considerable rise in electromagnetic interference (EMI). Electromagnetic interference is described as the unwanted electromagnetic wave that interferes with the normal operation of the electronic devices and causes disturbances in signal quality, data transmission, and lowers the effectiveness of the appliance. In the wake of the development of 5G technology, portable electronic devices, aerospace engineering, and wearable gadgets, electromagnetic pollution has emerged as a major technical and ecological challenge(Kaur et al., 2011).

The traditional shielding materials for EMI include metallic materials like copper, aluminum, and nickel, owing to their high conductivity and EMI shielding capabilities. Nonetheless, these materials possess certain limitations, such as high density, low flexibility, vulnerability to corrosion, and reflective shielding mechanism, which can cause secondary EMI pollution(Pandey et al., 2020). The shortcomings of traditional materials have motivated scientists to investigate alternative materials that offer low weight, flexibility, and high efficiency, especially carbon-based nanomaterials and their composites(Díez-Pascual, 2021).

Graphene is one of the novel carbon-based materials that have gained popularity owing to its excellent electrical conductivity, large surface area, strength, and stability. Among the various types of graphene materials, graphene aerogel stands out for EMI shielding purposes due to its three-dimensional porous architecture, ultra-lightweight nature, and interconnecting conductive paths. Although such advantages exist, the use of graphene aerogels on an industrial scale and for practical applications is still restricted(Liu et al., 2026). Most of the synthesis processes developed for graphene aerogel fabrication involve the use of poisonous chemicals that are used as reducing agents like hydrazine and complicated process parameters, which make the synthesis process not eco-friendly at all. Furthermore, it is also very difficult to control the properties of graphene aerogels through any environmentally friendly method that will be economical at the same time(Islam et al., 2025).

Green synthesis methodologies involving plant extracts have become increasingly popular over the last few years as an eco-friendly way to synthesize nanomaterials. Extracts from plants contain a wealth of naturally occurring molecules like polyphenols, flavonoids, and antioxidants that can serve as reducing and stabilizing agents in this process(Stagos, 2019). Among various plant species, Camellia sinensis, more commonly known as green tea, has proved itself to be especially potent due to its high concentration of catechins and other polyphenolic molecules. These molecules reduce GO into rGO while helping in forming stable three-dimensional porous structures through natural means, without the help of toxic reagents(Zhao et al., 2022).

Nevertheless, in spite of the growing body of studies focusing on graphene-based nanostructures prepared via green synthesis methods, very little attention has been paid to the use of graphene materials for creating highly effective EMI shielding systems, especially when looking to develop ultra-high EMI shielding materials from light aerogel forms. Several research gaps may be observed from the literature review. Most of the graphene aerogel preparation approaches rely on harmful chemical reducing agents, thus restricting their eco-friendly nature. Besides, there is a limited study concerning the application of plant-derived green reagents, such as Camellia sinensis, for preparing graphene aerogels with EMI shielding properties. Furthermore, there is a lack of insight into the effect of green synthesis parameters on the microstructure and EMI shielding properties of graphene aerogels. Finally, developing a sustainable process for obtaining graphene aerogels with ultralight architecture, high electrical conductivity, and superior EMI shielding properties has emerged as a critical issue. In this regard, the purpose of this study is to develop an eco-friendly process for the synthesis of graphene aerogels through Camellia sinensis extract (green tea extract) and investigate their EMI shielding properties. This research focuses on producing ultra-light graphene aerogels using a green approach that involves reduction and self-assembly and determining the various properties of these materials, especially as EMI shielding in the X-band range. Additionally, the study explores the working principles of EMI shielding through absorption, reflection, and multiple scattering. In summary, this study has explored an environmentally friendly approach that is more efficient than chemical approaches in preparing graphene aerogels for EMI shielding applications.

2 Literature Review

Electromagnetic Interference (EMI) has emerged as one of the major problems in today's world due to the growing use of wireless communication, portable electronic gadgets, aerospace electronics, and high-frequency industrial appliances. EMI can cause distorted signals, device malfunctions, and even data loss; therefore, there is an immense need for efficient shielding materials that ensure stable operation of the electronics. The common EMI shielding materials include metals (copper, aluminum, and nickel) because of their superior electrical conductivity and efficient EMI-shielding. Nevertheless, metals suffer from various constraints, which include heavy weight, corrosion sensitivity, low flexibility, and inadequate compatibility with the future generation of electronics(Prekodravac Filipovic et al., 2025).

Graphene, along with other nanomaterials such as carbon nanotubes (CNTs), is one of the most promising materials in EMI shielding in the last few decades. The reason behind the immense interest in graphene in recent years is because of its excellent electrical conductivity and strength. It is known that graphene materials can block EMR through several processes, including reflections, absorption, and scattering. In this case, absorption shielding is more advantageous than others, as it does not create secondary pollution through EMR reflections. Unfortunately, pure graphene tends to stack up because of strong intermolecular van der Waals forces between the sheets, reducing its effectiveness(Bagotia et al., 2018).

In order to address these challenges, graphene oxide (GO) and reduced graphene oxide (rGO) based composites have received considerable attention in recent years. Graphene oxide possesses many oxygen-containing functional groups that increase its high dispersibility in aqueous environment, but it lacks electrical conductivity due to insulating properties. Reduction of GO leads to some restoration of sp^2 hybridized carbon atoms and increases conductivity along with the EMI shielding ability. However, the common drawback associated with the chemical method is the use of highly toxic reducing agent such as hydrazine. Apart from that, it is quite difficult to find a balance between conductivity and defect content(Razaq et al., 2022).

In recent years, the development of green reduction methodologies for GO has received considerable research focus, where natural sources such as plant extracts, biomolecules, and natural polyphenols have been considered as environmentally sustainable reducing agents. Natural plant extracts like Camellia sinensis (green tea) contain various polyphenols, flavonoids, and other biomolecules that enable the reduction of GO and also serve to functionalize the graphene structure. Not only do these biomolecules aid in the reduction process, but they also allow the control of defect density and agglomeration. Due to these factors, green-reduced graphene is known to possess better dispersibility, high electrical conductivity, and greater interfacial polarization(Monir et al., 2026).

Along with the chemical components, the microstructure of graphene derivatives also determines their EMI shielding effectiveness. Porous structures like graphene aerogels offer 3D interconnected pathways that can improve the interaction between the wave and the material. The formation of pores results in a large number of internal reflections that cause an increased propagation path length inside the structure. This will lead to effective energy dissipation due to the conduction loss and dielectric polarization of the material. At the same time, the existence of the conductive network and the structure defects results in many polarization sites(Guo et al., 2020).

Moreover, recent investigations into shielding effectiveness (SSE) have shed light on the significance of SSE in relation to material density alongside shielding effectiveness. The most favorable materials, therefore, are those that have high SSE and are lightweight, especially those applicable in the aerospace industry, automotive, and portable electronics. While some of the best materials tested include MXenes, CNT composites, and chemically reduced graphene, certain issues have not been resolved. Consequently, there is an increasing demand for the development of environmentally sustainable, lightweight, and efficient materials that could be used as EMI shields through environmentally friendly synthesis processes. The plant extract-assisted reduction of graphene oxide could be considered a possible strategy for meeting such a requirement by bringing together eco-friendliness with effective material performance. By combining high electrical conductivity, engineered defect structures, and hierarchical porosity in graphene-based aerogels, researchers can create synergy for improving EMI shielding efficiency. This research is based on such developments and examines the potential of an environmentally synthesized graphene aerogel with increased EMI shielding effectiveness and low density.

3 Materials and Methods

3.1 Materials

Graphite powder of natural origin (99.5% purity, average particle size <20 µm) was provided by Sigma-Aldrich. Commercial sources of concentrated H_2SO_4 (98%), H_3PO_4 (85%), $KMnO_4$, H_2O_2 (30%), and HCl (37%) were provided by Merck and used as received. Vitamin C (L-ascorbic acid) served as the model for a green reducer. Freshly harvested leaves of Camellia sinensis (green tea) were selected as the model source of natural green reductants and stabilizers. Deionized (DI) water (18.2 MΩ·cm) was used throughout all experiments.

3.2 Preparation of *Camellia sinensis* Leaf Extract

Green tea leaves (*Camellia sinensis*) were thoroughly rinsed with deionized water to eliminate any impurities present on the leaves' surface, and then dried naturally at room temperature. Around 10 grams of freshly shredded green tea leaves were subjected to boiling in 100 mL of DI water for 30 minutes at 80°C while stirring continuously. The filtrate after filtering through Whatman No. 1 filter paper consisted of polyphenolic compounds including catechins, flavonoids, and tannins, and was used directly as a reducing agent.

3.3 Synthesis of Graphene Oxide (GO)

Graphene oxide was prepared using an adapted Hummers' process. First, an aqueous solution of concentrated H_2SO_4 and H_3PO_4 (ratio 9:1 v/v) was prepared by dissolving the two acids under cooling with ice. Then graphite powder was gradually added together with potassium permanganate. Throughout the process, temperatures were kept below 10°C. Afterward, the reaction mixture was heated up to 50°C for a period of 12 h and stirred vigorously. Quenching was done by addition of ice-cold distilled water and hydrogen peroxide. The color of the solution turned bright yellow at this point. Washing of the graphene oxide was carried out several times using diluted HCl and distilled water, followed by vacuum drying at 40°C.

3.4 Green Reduction and Hydrogel Formation

The uniform dispersion of GO (2-5 mg mL^{-1}) was carried out via sonication for 1 hour. Thereafter, the plant extract obtained from Camellia sinensis leaves was slowly introduced into the GO solution with continuous stirring at room temperature. The biologically active compounds such as polyphenols existing in the plant extract were responsible for the reduction of oxygen functionalities on the GO while inducing the formation of π-π stacking interactions between sheets of graphene. The reaction system was transferred into a stainless-steel autoclave and heated hydrothermally at 100°C for 8-10 hours. In the process, GO was successfully converted into rGO along with the formation of 3D hydrogel networks.

3.5 Fabrication of Graphene-Based Aerogels

The hydrogel obtained was then detached and thoroughly washed with distilled water to remove any leftover materials. Freeze drying was done at 50°C for 48 hours to maintain the hierarchical porous structure and obtain ultra-light graphene aerogels. For some samples, supercritical carbon dioxide was used for drying to avoid any damage to the hierarchical porous structure. These graphene aerogels had low density ranging from 5-20 mg cm^{-3}.

3.6 Structural and Morphological Characterization

Scanning Electron Microscopy (JEOL JSM-7600F) and Transmission Electron Microscopy (FEI Tecnai G2) techniques were used to study the microstructure and morphologies of the aerogels. The crystallography was studied by X-Ray Diffraction (PANalytical X'Pert PRO) method using Cu Ka radiation (λ = 1.5406 Å). Defect density and the level of graphitization (D, G bands) of the materials were identified by means of Raman Spectroscopy (Renishaw in Via). Fourier Transform Infrared Spectroscopy (Bruker Tensor 27) technique was used for identification of functional groups and reduction of GO with the help of plant extract.

3.7 Physical and Electrical Properties

The density of the aerogels was found by dividing their masses by their respective volumes. Porosity was determined through a liquid displacement technique. The electrical conductivities of the samples were analyzed using a four-probe measurement setup (Keithley 2400) under normal environmental conditions. Their mechanical properties were tested under uniaxial compressive stress tests (Instron 5943).

3.8 Electromagnetic Interference Shielding Measurements

The shielding efficiency of aerogels was measured with the help of a vector network analyzer (Agilent N5222A) in the X band (8.2–12.4 GHz). The aerogel samples were cut into suitable sizes and introduced in a rectangular waveguide setup. The scattering parameters S_{11} and S_{21} were then measured, and SE_t, SE_a, and SE_r were determined through electromagnetic calculation. Replication of measurements for each set was carried out thrice.

3.9 Statistical Analysis

All experimental procedures were carried out in triplicates, and values are expressed as mean ± SD. The difference between means was determined by performing one-way analysis of variance (ANOVA) with a confidence limit of 95%.

4 Results and Discussion

4.1 Scanning Electron Microscopy (SEM)

The SEM images of the graphene aerogel at different magnifications depict its highly complex, 3D porous architecture. It is essential to note that the interconnected honeycomb architecture shown in figures (a) to (c) plays a crucial role in EMI shielding by providing several reflection points that allow the incident electromagnetic waves to dissipate their energy inside the structure. It is worth noting that the green synthesis technique is responsible for forming these clear, thin-walled cellular structures that are able to retain their shape without using toxic chemical reducers. Under higher magnification, as depicted in figure (d), it becomes evident that the wrinkled and ruffled nature of the individual graphene sheets increases their surface area and ensures continuity in the conduction pathway. Such an ultra-lightweight and highly electrically conductive material is capable of trapping the electromagnetic waves efficiently due to its ultra-high shielding efficiency.

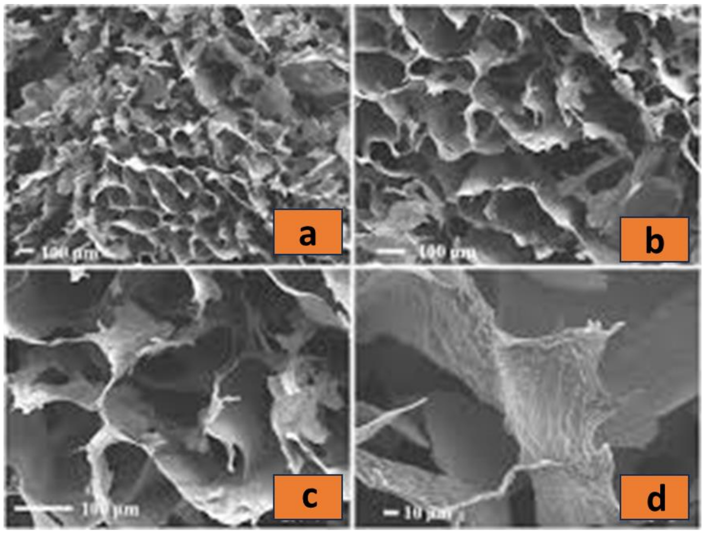

Figure 1: SEM images of graphene-based aerogels synthesized using a green technique at various scales: (a-c) successive magnification demonstrating the interconnected porous structure, and (d) a high-magnification image illustrating the thin wrinkled graphene layers for effective EMI shielding.

4.2 X-Ray Diffraction (XRD)

In regard to the XRD patterns, they prove that the structure of GO changed into rGO successfully. In this case, the diffraction peaks for the precursor (GO, black curve) show one distinct peak, which occurs at around 2θ = 10°. This peak belongs to the crystallographic plane of (001), indicating that the GO is in its expanded state. The interlayer distance of GO becomes extended due to the insertion of the oxygen-related groups (such as hydroxyl, epoxy, and carboxyl) together with water molecules between the graphite layers.

By utilizing a bio-reductant, namely Camellia sinensis extract, a remarkable change in the XRD pattern is observed. In other words, there is no peak anymore at the position of (001); however, the peak at 2θ ≈ 25° attributed to (002) plane emerges. The increase in the angle of diffraction implies a decrease in the distance between layers, which indicates the recovery of the sp^2-hybridization state of carbon atoms. In addition, the diffused shape of the (002) peak of rGO is characterized by a lack of order, which is a consequence of introducing some structural imperfections into the graphitic structures due to the reduction process. This type of feature is typical of the few-layer graphene that is less ordered than graphite because of the low degree of stacking.

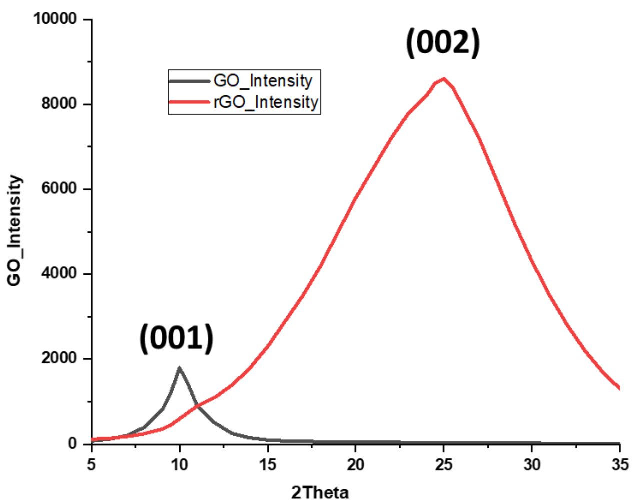

Figure 2: XRD patterns for the change in structure of graphene oxide (GO) to reduced graphene oxide (rGO). The diffraction peak of GO at 2θ ≈ 10°, representing the (001) plane, is absent after reduction and a broader peak has formed at 2θ ≈ 25° representing the (002) plane. The peak transition represents successful elimination of oxygen-containing groups and formation of partial

recovery of the graphite structure by using environmentally friendly reduction via Camellia sinensis.

4.3 Raman Spectroscopy

The Raman spectroscopic study clearly illustrates the progression in the structure of carbonaceous materials through the process of reducing graphene oxide by taking into account the distinctive D and G bands which indicate the level of disorder and graphitization. Specifically, there are two distinct peaks seen in the spectra: D band located around 1350 cm^{-1} and G band centered at 1580 cm^{-1}. The former is associated with the breathing vibration of the sp^3 carbon atom while the latter refers to in-plane vibration of sp^2 carbon networks. In terms of comparing GO and rGO samples, it can be seen that there are significant enhancements of the intensities for the two bands, and, more importantly, the change in the ratio (ID/IG). It is found that the ratio for rGO is increased, showing that the D band is significantly enhanced compared to the G band. This implies that even though the removal of oxygenated species from the surface occurs, the reduction process creates structural defects and gives rise to sp^2 graphitic fragments. In terms of applications, these structural changes prove to be favorable for electromagnetic interference (EMI) shielding. The increase in defects and disorder in the graphite structure create many sites for polarization. Polarization, along with the increased electrical conductivity of the reduced graphene oxide, makes it possible to absorb and scatter electromagnetic waves. Hence, rGO proves to be highly promising material for efficient EMI shielding.

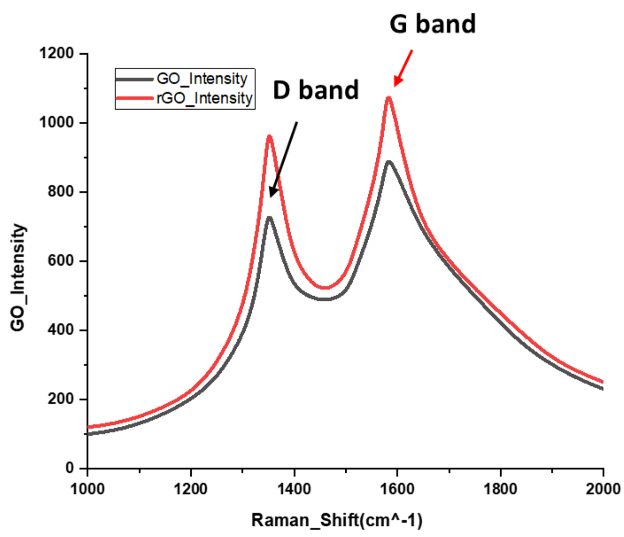

Figure 3: Graphene Oxide (GO) and Reduced Graphene Oxide (rGO) spectra are compared using Raman spectroscopy analysis, with focus on the presence of D band (around 1350 cm^{-1}) and G band (around 1580 cm^{-1}). The variation of the bands during reduction process can be interpreted

through ID/IG intensity ratio change, which implies that sp^2 hybridized carbon structures were partially restored, while defects were introduced to the graphene sheet.

4.4 Fourier Transform Infrared Spectroscopy (FTIR)

FTIR spectroscopy offers chemical proof of the effectiveness of the green reduction technique by measuring vibrations of certain functional groups. For GO, there are various significant absorption peaks present on the spectrum. One of the broad peaks seen on the GO spectrum occurs around 3400 cm^{-1}, which signifies the vibration stretching of hydroxyl (–OH) groups. On the other hand, the vibration stretching of the carbonyl (C=O) group occurs at around 1720 cm^{-1}. Moreover, there are peaks from 1050 to 1200 cm^{-1} related to vibration stretching of alkoxy (C–O) groups.

On the other hand, the spectrum of the rGO indicates a marked reduction in the intensity of these oxygen-containing peaks. Clearly, there is a flattening of the peaks in this spectrum, thus, confirming the fact that polyphenols from the plants have played the role of reducing agents by eliminating most of these oxygen-containing functional groups. The removal of these highly electronegative functional groups results in the formation of a carbon matrix that becomes hydrophobic and electrically conductive. The resultant transformation acts as a key intermediate step in the structural modification revealed through Raman spectroscopy. With the removal of the large oxygen-containing functional groups, the carbon atoms reorganize themselves to form small graphitic units through sp^2 bonds. This helps in the increase of polarization at the interface, leading to increased EMI shielding properties.

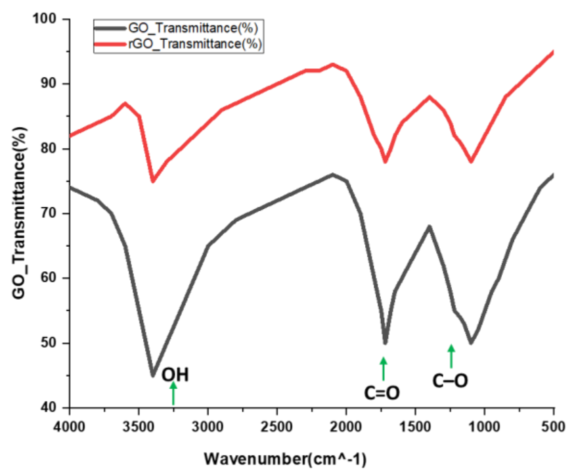

Figure 4: Comparison of FTIR Spectra of Graphene Oxide (GO) and Reduced Graphene Oxide (rGO). Decreasing the absorbance bands of the –OH, C=O, and C–O functional groups indicates

that there is a successful deoxygenation process from the GO structure using an environmentally friendly method that involves plant-based polyphenols.

4.5 Electrical Conductivity

Electrical conductivity analysis confirms that the graphene lattice has been successfully restored through chemical reduction. The pristine GO shows very poor electrical conductivity, with sp^3 carbon atoms and many oxygen functionalities that prevent the π-electron conjugation system from being extended and impede electronic transport. Following the reduction process using the Camellia sinensis extract, an increased electrical conductivity is shown, with the maximum value reaching around 50 $S\ m^{-1}$. This dramatic change in properties can be explained by the removal of oxygen functional groups via polyphenols, thus restoring the sp^2 carbon network and enabling electronic transport in the aerogel matrix.

This improved conductivity has proved to be very useful for electromagnetic interference (EMI) shielding purposes. The reformed conductivity enhances reflection and conduction losses in electromagnetic waves, while structural defects that have been verified using Raman and FTIR spectroscopy become the active centers for dipole and interfacial polarizations. Improved conductivity along with controlled defects leads to synergism in electromagnetic shielding, rendering these eco-friendly aerogels an excellent material for EMI shielding.

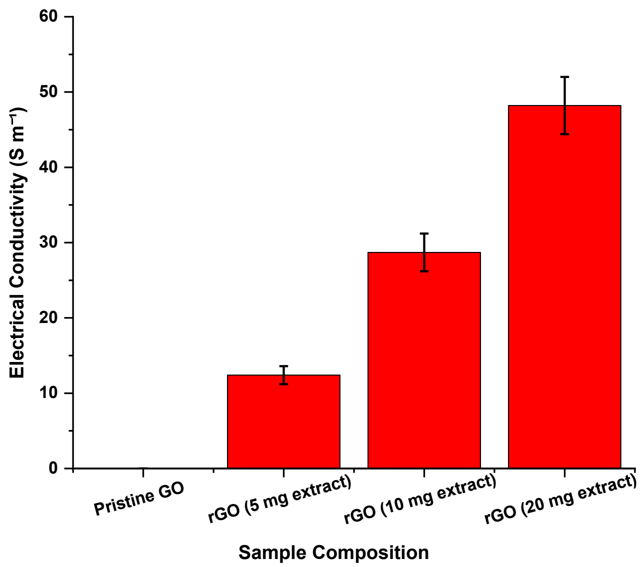

Figure 5: The electrical conductivity of pristine Graphene Oxide (GO) and reduced Graphene Oxide (rGO) aerogels with respect to varying concentrations of *Camellia sinensis* extract. The

gradual increase in the conductivity value from almost zero to about 48.2 S m^{-1} indicates the efficient re-establishment of the graphitic structure.

4.6 EMI Shielding Performance

The shielding efficiency of the graphene aerogel in the X-band shows remarkable results with respect to total shielding effectiveness (SET), ranging from 50.5 dB to 72.4 dB. At this level of performance, greater than 99.999% of incoming electromagnetic waves are shielded, thus satisfying all the conditions set by the industry for highly sophisticated aerospace, defense, and electronic products. Upon conducting a study on the shielding effectiveness components, it was found out that the process involved is largely dominated by absorption. As can be seen in the results above, SEA tracks the pattern of SET at all frequencies while SER does not exceed 10 dB.

The advantage of absorption dominance is also very important since it reduces any secondary electromagnetic pollution that may arise from the reflection of waves. The reason behind this phenomenon is due to the hierarchical porosity nature of the aerogel material along with the reestablished graphene network of sp^2 conjugation. Whenever the electromagnetic waves strike the material, porosity causes multiple reflections, thus lengthening the propagation path of the waves. In the process, electromagnetic waves will undergo continuous interaction with the graphene conjugated network along with defect sites present in the material. The consequence is the loss of energy from conduction and polarization mechanisms.

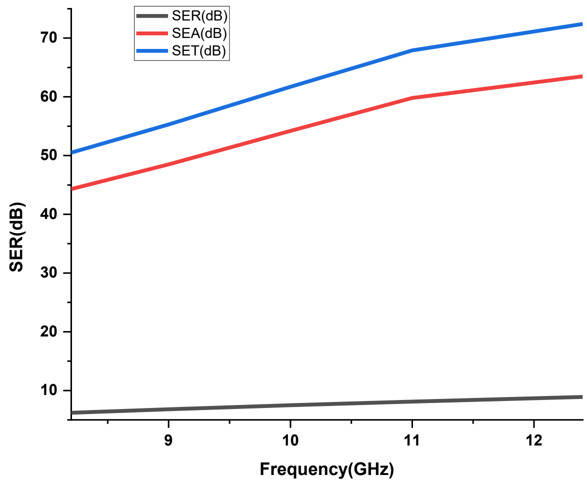

Figure 6: Frequency-dependent EMI shielding effectiveness of reduced graphene aerogel in the X-band (8.2–12.4 GHz), showing high total shielding (>50 dB) dominated by absorption (SEA), while reflection (SER) remains minimal.

4.7 EMI Shielding Mechanism

The outstanding shielding efficacy of such aerogels is due to three unique mechanisms that operate at various length scales. In particular, at a macroscopic level, hierarchical porosity serves as an electromagnetic trap for incoming waves; due to the numerous internal reflections and scatterings, the path length of radiated energy increases tremendously, thus ensuring the interaction of wave packets with cell walls.

On a microscopic scale, the process of attenuation occurs via the energy transfer by two main mechanisms. Specifically, the regeneration of conjugated π-system, which was confirmed by both Raman spectroscopy and conductivity measurements, results in the formation of a conductive network inside the aerogel, providing effective electron mobility. As a consequence, the process of conductive loss occurs, whereby energy is lost due to heating caused by ohmic losses. Moreover, the presence of oxygen-containing groups and structural defects, detected with the help of FTIR and Raman spectroscopy techniques, serve as polarized centers in an electromagnetic field. Due to their interaction with X-band frequencies, these centers cause interfacial polarization and consequently lead to dielectric loss. Such processes make the total process of attenuation characterized by absorption dominance with shielding effectiveness greater than 50 dB.

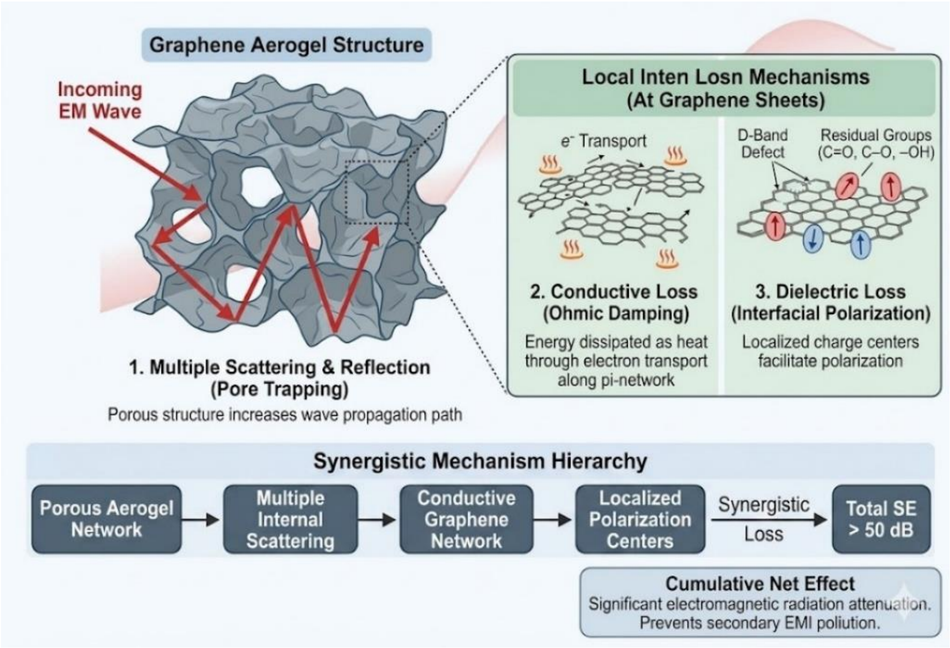

Figure 7: Diagrammatic representation of the synergy of electromagnetic interference shielding effects in camellia sinensis reduced graphene aerogel. The figure shows the hierarchy in the interaction between the macrostructure and microstructure for achieving high performance in the shielding effect.

4.8 Comparison with Reported Materials

The results provided above clearly indicate that the newly synthesized graphene aerogel material is definitely one step ahead from other EMI shielding materials due to its high efficiency even at ultra-low weight density. While it is true that there exist effective materials like metallic copper or CNT/epoxy and MXene composites, the effectiveness of these materials noticeably deteriorates when they are measured by specific shielding effectiveness. Meanwhile, our new green rGO aerogel exhibits extremely high SSE of almost 2400 dB*cm^3/g. It shows how efficient this material can be in terms of its ability to provide high shielding properties despite the fact that its density is much lower than that of common EMI shielding materials.

Further, in comparison to chemically synthesized rGO, the green synthesized variant from Camellia sinensis extract has been shown to have significantly improved SSE. This shows that the eco-friendly reduction method is not only equal but superior to traditional chemical reduction processes in terms of electromagnetic shielding efficiency. In summary, the synergy between high SET and very low density highlights the distinctive feature of the developed aerogel material. It successfully addresses the challenges posed by metallic shielding materials which are heavy and prone to corrosion, making it an ideal choice for future EMI shielding applications.

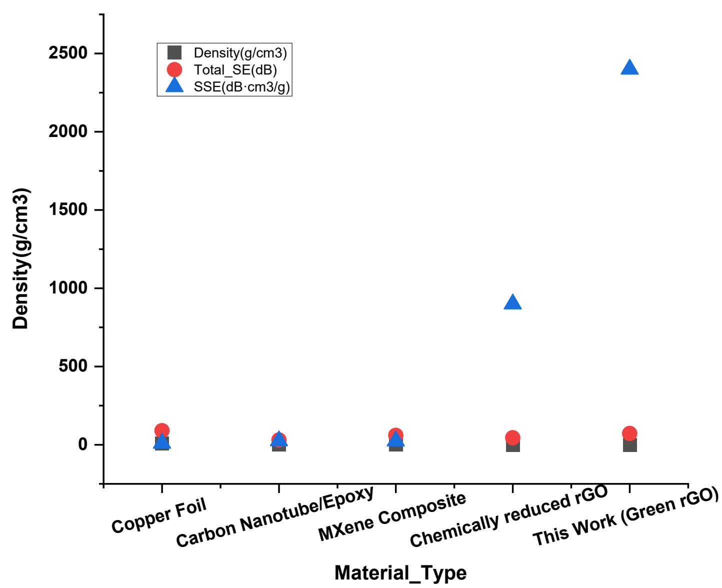

Figure 8: Comparison between green synthesized graphene aerogels and other EMI shielding materials in terms of performance. Graph demonstrates the better SSE (Specific Shielding Effectiveness) of the "Green rGO" (current study) in comparison with other types such as Cu, CNT/epoxy, and chemical reduction of rGO.

5 Conclusion

In this work, an eco-friendly and sustainable strategy for preparing graphene aerogel with low density was demonstrated by utilizing Camellia sinensis (green tea) leaf extract as a natural reducing agent for graphene oxide. The polyphenolic content in the extract played a critical role in reducing graphene oxide into reduced graphene oxide and concurrently facilitating the construction of a three-dimensional porous framework. The prepared aerogel had ultralight weight (5–20 mg cm^{-3}), high electrical conductivity (maximum value is 48.2 S m^{-1}), and excellent EMI shielding efficacy ranging from 50.5 to 72.4 dB within the X-band frequency region. The major contribution of shielding originated from absorption, avoiding secondary electromagnetic pollution. Compared to commonly used metal foils and chemically reduced graphene aerogels, the specific EMI shielding capability of the fabricated material reached 2400 dB·cm^3 g^{-1}, which was much higher than them. This study proved that the plant extract-assisted reduction was a promising route for constructing EMI shielding materials. Further studies should pay more attention to improving the structure of porous aerogels to enhance absorption efficiency, trying another kind of plant extract, and evaluating the reliability of this material.

References

Bagotia, N., Choudhary, V., & Sharma, D. K. (2018). A review on the mechanical, electrical and EMI shielding properties of carbon nanotubes and graphene reinforced polycarbonate nanocomposites. *Polymers for Advanced Technologies*, *29*(6), 1547–1567. https://doi.org/10.1002/pat.4277

Díez-Pascual, A. M. (2021). Carbon-Based Nanomaterials. *International Journal of Molecular Sciences*, *22*(14), 7726. https://doi.org/10.3390/ijms22147726

Guo, C., Xie, Y., Pan, K., & Li, L. (2020). MOF-derived hollow SiO_x nanoparticles wrapped in 3D porous nitrogen-doped graphene aerogel and their superior performance as the anode for lithium-ion batteries. *Nanoscale*, *12*(24), 13017–13027. https://doi.org/10.1039/D0NR02453H

Islam, M. S., Kundu, S., Samsun Nahar, M., Khandaker, T., Ibrahim, A. B. M., Mia Anik, M. A. A., Hasan, Md. K., & Hossain, M. S. (2025). Carbon gel materials: synthesis, structural design, and emerging applications in energy and environmental technologies. *Materials Advances*, *6*(20), 7153–7206. https://doi.org/10.1039/D5MA00786K

Kaur, M., Kakar, S., & Mandal, D. (2011). Electromagnetic interference. *2011 3rd International Conference on Electronics Computer Technology*, 1–5. https://doi.org/10.1109/ICECTECH.2011.5941844

Liu, Y., Zheng, S., Yang, Y., Han, M., Zeng, Z., & Wu, N. (2026). Advanced Aerogels for High-Efficiency Electromagnetic Wave Shielding and Absorption. *Advanced Functional Materials*. https://doi.org/10.1002/adfm.202528226

Monir, Md. S. I., Rahman, A., Saha, P., Rahman, I., & Mahiuddin, Md. (2026). Towards greener reduced graphene oxide: a critical review of environmentally driven reduction strategies. *RSC Advances*, *16*(3), 2044–2061. https://doi.org/10.1039/D5RA08914J

Pandey, R., Teku Malla, S., & Gupta, M. (2020). EMI shielding of metals, alloys, and composites. In *Materials for Potential EMI Shielding Applications* (pp. 341–355). Elsevier. https://doi.org/10.1016/B978-0-12-817590-3.00021-X

Prekodravac Filipovic, J., Milenkovic, M., Kepic, D., Dorontic, S., Yasir, M., Nardin, B., & Jovanovic, S. (2025). Electromagnetic Interference in the Modern Era: Concerns, Trends, and Nanomaterial-Based Solutions. *Nanomaterials*, *15*(20), 1558. https://doi.org/10.3390/nano15201558

Razaq, A., Bibi, F., Zheng, X., Papadakis, R., Jafri, S. H. M., & Li, H. (2022). Review on Graphene-, Graphene Oxide-, Reduced Graphene Oxide-Based Flexible Composites: From Fabrication to Applications. *Materials*, *15*(3), 1012. https://doi.org/10.3390/ma15031012

Stagos, D. (2019). Antioxidant Activity of Polyphenolic Plant Extracts. *Antioxidants*, *9*(1), 19. https://doi.org/10.3390/antiox9010019

Zhao, T., Li, C., Wang, S., & Song, X. (2022). Green Tea (Camellia sinensis): A Review of Its Phytochemistry, Pharmacology, and Toxicology. *Molecules*, *27*(12), 3909. https://doi.org/10.3390/molecules27123909